

Accepted Manuscript

Optimized photoluminescence properties of a novel red phosphor $\text{LiSrAlF}_6:\text{Mn}^{4+}$ synthesized at room-temperature

Mengmeng Zhu, Yuexiao Pan, Mingmei Wu, Hongzhou Lian, Jun Lin



PII: S0925-8388(18)33412-1

DOI: [10.1016/j.jallcom.2018.09.172](https://doi.org/10.1016/j.jallcom.2018.09.172)

Reference: JALCOM 47591

To appear in: *Journal of Alloys and Compounds*

Received Date: 26 July 2018

Revised Date: 11 September 2018

Accepted Date: 15 September 2018

Please cite this article as: M. Zhu, Y. Pan, M. Wu, H. Lian, J. Lin, Optimized photoluminescence properties of a novel red phosphor $\text{LiSrAlF}_6:\text{Mn}^{4+}$ synthesized at room-temperature, *Journal of Alloys and Compounds* (2018), doi: <https://doi.org/10.1016/j.jallcom.2018.09.172>.

This is a PDF file of an unedited manuscript that has been accepted for publication. As a service to our customers we are providing this early version of the manuscript. The manuscript will undergo copyediting, typesetting, and review of the resulting proof before it is published in its final form. Please note that during the production process errors may be discovered which could affect the content, and all legal disclaimers that apply to the journal pertain.

Optimized photoluminescence properties of a novel red phosphor**LiSrAlF₆:Mn⁴⁺ synthesized at room-temperature**

Mengmeng Zhu,^a Yuexiao Pan,^{a*} Mingmei Wu,^c Hongzhou Lian,^b Jun Lin^{b*}

^a*Nanomaterials and Chemistry Key Laboratory, Faculty of Chemistry and Materials Engineering, Wenzhou University, Zhejiang Province, Wenzhou 325027, P. R. China.*

Tel. & Fax: (+86) 577-8837-3017. E-mail: yxpan8@gmail.com;

^b*State Key Laboratory of Rare Earth Resource Utilization, Changchun Institute of Applied Chemistry, Chinese Academy of Sciences, Changchun 130022, P. R. China.*

Fax: +86-431-85698041; Tel: +86-431-85262031. E-mail: jlin@ciac.ac.cn;

^c*MOE Key Laboratory of Bioinorganic and Synthetic Chemistry/ School of Chemistry and Chemical Engineering, Sun Yat-Sen University, Guangzhou 510275, P.*

R. China. Tel: 86-20-84111823 (Office). E-mail: ceswmm@mail.sysu.edu.cn

Abstract

A red phosphor with a broad excitation band in blue and sharp emission peaks in red is needed for compensating the red components of white light-emitting diodes (WLEDs) by converting blue light with a yellow phosphor $\text{Y}_3\text{Al}_5\text{O}_{12}:\text{Ce}^{3+}$ (YAG:Ce). The red phosphor $\text{LiSrAlF}_6:\text{Mn}^{4+}$ (LSAF:Mn) with morphology of flaky particles about 50 μm in diameter has been synthesized by an ion-exchange reaction route at room-temperature in air. The as-synthesized phosphors were characterized by x-ray powder diffraction (XRD), scanning electron microscope (SEM), and temperature-dependent photoluminescence (PL) spectra. The excitation spectrum of LSAF:Mn shows a broad-band excitation from 400 to 500 nm that is due to the spin-allowed transition of ${}^4\text{A}_{2g} \rightarrow {}^4\text{T}_{2g}$ of Mn^{4+} , indicating a potential application for solid state lighting. The optimal PL intensity of the phosphor LSAF:Mn has been obtained by optimizing the synthetic parameters.

1. Introduction

WLEDs have attracted much attention due to their high efficiency, long serving time, and environmental friendly compared to conventional incandescent and fluorescence lightings.¹⁻³ The main strategy to obtain WLEDs is mixing the blue light from InGaN LED chips and yellow light from phosphors YAG:Ce, which suffers from the problems of low color rendering index (CRI < 80) and high correlated color temperature (CCT > 5000 K) because of the insufficient red contribution in their white PL spectra.⁴⁻⁹ Combination of a red phosphor to compensate the red component is a feasible approach to obtain white light with controlled emission color properties and a CRI higher than 90.⁴⁻⁹ In this regard, it is essential to develop red phosphors that can be efficiently excited by the blue LED chips.

To develop a novel efficient red-emitting phosphors being excitable by blue LED, Mn^{4+} with outer $3d^3$ electron configuration exhibiting narrow-band emission lines in red region and a broad-band excitation in blue region are considered to be efficient candidate because the Mn^{4+} doped red phosphors can be effectively excited by blue light and emit intense red luminescence.¹⁰⁻²¹ Generally, Mn^{4+} ions located at the centers of octahedral sites in solid state inorganic compounds act as luminescence emitters. Mn^{4+} ions in most hosts of red phosphors have a group of sharp emitting peaks in red region between 600 and 650 nm. The fine structure of the emission spectrum and the efficiency of the Mn^{4+} doped phosphors are strongly dependent on the microenvironment Mn^{4+} experienced that including the crystallography structure, coordination environments, and remote neighbouring-cations.¹⁰⁻¹⁴ For example, a red phosphor $\text{Rb}_2\text{SiF}_6:\text{Mn}^{4+}$ obtained by replacement of K^+ with Rb^+ shows better thermal stability than $\text{K}_2\text{SiF}_6:\text{Mn}^{4+}$.¹⁰ We have reported the formation mechanism and the luminescence properties of Mn^{4+} -substituted phosphors containing $[\text{GaF}_6]^{3-}$ and

$[\text{AlF}_6]^{3-}$ octahedrons in $\text{Li}_3\text{Na}_3\text{Ga}_2\text{F}_{12}$ (LNGF) and $\text{Li}_3\text{Na}_3\text{Al}_2\text{F}_{12}$ (LNAF), respectively.^{11,12} It is observed that the PL spectra of LNGF:Mn are very similar to those of LNAF:Mn but the quantum yield of LNGF:Mn is nearly 3 times of that of LNAF:Mn. Moreover, the luminescence color purity and luminescence efficiency of $\text{K}_2\text{NaAlF}_6:\text{Mn}^{4+}$ are much better than those of $\text{K}_2\text{LiAlF}_6:\text{Mn}^{4+}$ due to slight nephelauxetic effect in K_2NaAlF_6 .^{13,14} Thus, the performance of the Mn^{4+} -substituted phosphors is strongly subject to the surroundings of the luminescence center in host lattice.

To our knowledge, the preparation and optical properties of Mn^{4+} doped alkaline earth metal fluoride phosphors have not been reported so far except for $\text{BaTiF}_4:\text{Mn}^{4+}$ and $\text{BaSiF}_4:\text{Mn}^{4+}$.¹⁵⁻¹⁷ Additionally, there is no Mn^{4+} doped alkaline earth metal fluoride phosphors containing Sr^{2+} or Ca^{2+} reported previously. In this work, a novel red Mn^{4+} doped hexa-fluoroaluminate LSAF:Mn has been firstly synthesized by the ion-exchange method at room-temperature and its formation mechanism has been discussed. The phosphor LSAF:Mn shows red sharp-peaky emission, a broad absorption in the blue light region, and excellent thermal stability, which is promising in improvement of the performance of WLEDs based on InGaN chips and YAG:Ce phosphors. This work will open the opportunity for development of novel Mn^{4+} doped fluoride phosphors containing alkaline earth metal.

2. Experimental

2.1 Synthesis of red phosphors

Starting materials

The raw materials used in this work include KMnO_4 , KHF_2 , H_2O_2 (30 wt%), LiF , SrCO_3 , AlF_3 , HF (40 wt%) and ethyl alcohol (AR). All of thesis starting reagents were

used directly without any further purification. All the chemicals were purchased from Aladdin Reagent Co., Ltd (Shanghai).

Synthesis of K_2MnF_6

According to the operating procedures reported previously, 230 mmol KHF_2 and 5.7 mmol $KMnO_4$ were dissolved in 30 mL HF (40 wt%) solution, then 0.6 ml H_2O_2 (30 wt%) was dropwise added.²² After 30 min magnetically stirring, the deep purple solution gradually turned yellow and a yellow precipitate was obtained at the same time. The resulting yellow solid product K_2MnF_6 was collected carefully by sucking filtration, washed extensively with methanol several times, and dried at 60 °C for 4 hours.

Synthesis of host lattice $LiSrAlF_6$

Herein, 0.01 mol LiF, 0.01 mol $SrCO_3$, and 0.01 mol AlF_3 were weighed and dissolved in 20 ml HF (10 wt%) solution under stirring. The white precipitate of $LiSrAlF_6$ was produced at room-temperature after stirring for 4 h. The resulting white solid compounds were filtered, washed with ethyl alcohol, and dried at 60°C for 4 h.

Synthesis of red phosphor $LiSrAlF_6:Mn^{4+}$

Red phosphors $LiSrAlF_6:Mn^{4+}$ were prepared via an ion exchange and co-precipitation combined synthesis with different molecular values of $K_2MnF_6/LiSrAlF_6$. In a typical synthesis, 0.2 mmol K_2MnF_6 was added into 20 ml 10 wt % HF solution until completely dissolved, and 10 mmol $LiSrAlF_6$ was added into the yellow transparent solution. After magnetically stirring for 3 hours, the precipitates were collected, washed with ethyl alcohol for several times, and dried at 60 °C for 4 hours.

2.2 Characterization

XRD patterns of the products were collected on a Bruker (Karlsruhe, Germany) D8 Advance x-ray powder diffraction (XRD) with graphite monochromatized Cu K_{α} radiation ($\lambda = 0.15418$ nm) at the scan rate of $10^{\circ}.\text{min}^{-1}$ in the two degrees range from $10^{\circ} \sim 80^{\circ}$. The morphology and elemental composition of the as-prepared products were studied by a Nova NanoSEM 200 scanning electron microscope (FE-SEM, FEI Inc.) with an attached energy-dispersive x-ray spectrum (EDS), transmission electron microscopy (TEM), and selected area electron diffraction (SAED), elemental compositions analysis obtained using an energy dispersive spectrometer (EDS) with a JEOL 2100F high-resolution transmission electron microscope using an accelerating voltage of 200 kV. The thermal stability the red phosphors are investigated by thermogravimetrics (TG) analysis and differential scanning calorimeter (DSC; Netzsch STA 449 C, at a heating rate of $10 \text{ K}.\text{min}^{-1}$). UV-vis diffuse reflectance spectra were measured by using a Shimadzu UV-3600 spectrometer. Photoluminescence (PL) spectra were recorded on FluoroMax-4 spectrofluorometer (Horiba Jobin Yvon Inc.) with a 150 W xenon lamp (as the excitation source) with a heating attachment.

3. Results and discussions

3.1. Phase purity, morphology and composition analysis

The phase purities of the products prepared at different temperatures and with various molecular ratios of $\text{K}_2\text{MnF}_6/\text{LiSrAlF}_6$ by keeping other reaction conditions consistent, have been characterized using XRD as shown in Fig. 1. All of the strong and sharp diffraction peaks of the samples LSAF:Mn obtained at temperatures from

room-temperature to 200 °C and with $K_2MnF_6/LiSrAlF_6$ ranging from 0.5 to 16 mol% can be indexed as a pure hexagonal LSAF phase. All the locations and relative intensities of the diffraction peaks coincide well with the values in standards card (ICDD No.48-1640) of LSAF. No other impurity phase can be observed, which indicates that the pure hexagonal phase LSAF can be readily prepared using this method. The formation of the LSAF precipitate can be expressed as following:



The red phosphor LSAF:Mn has been obtained through ion exchange and the partial anions $[AlF_6]^{3-}$ were replaced by $[MnF_6]^{2-}$ when mixing K_2MnF_6 and LSAF in HF solution based on the following reactions:



In order to further study the crystal structure information of the obtained phosphors, the Rietveld refinement of LSAF:Mn with the single crystal structure data of LSAF (ICSD No. 68905) as the initial model was carried out using the General Structure Analysis System (GSAS) program, and the result is shown in Fig. 2a. The black line represents the difference between experimental and calculated, and the blue sticks mark the Bragg reflection position. It shows that they match very well with that obtained from the experimental curve, indicating that the doped Mn^{4+} ions does not cause any impurity in the LSAF host structure.

The final refinement structural parameters and the the atom coordinates are summarized in Table 1. It demonstrate that LSAF:Mn belong to hexagonal structure with a group of P-31c(163). The unit-cell parameters are $a = b = 5.071 \text{ \AA}$, $c = 10.189$

\AA , $\alpha = \beta = 90^\circ$, $\gamma = 120^\circ$ and $V = 226.91 \text{ \AA}^3$, $N = 2$. The final results of refinement are converged to $R_{wp} = 5.24\%$ and $R_p = 11.14\%$, indicating good refinement quality and the formation of a single-phase of LSAF. According to the Rietveld refinement result, the crystal structure is drawn using Diamond software and shown in Fig. 2b. In the crystal lattice and the unit cell of LSAF, each Al^{3+} is surrounded by 6 F^- ions to form a regular $[\text{AlF}_6]^{3-}$ octahedral structure. In HF acid solution, the partly exchange between ions $[\text{MnF}_6]^{2-}$ and $[\text{AlF}_6]^{3-}$ occurs during stirring, and the Mn^{4+} ions were stabilized at the lattice sites of Al^{3+} ions.

The corresponding histograms of size distribution for the LSAF:Mn is depicted in Fig. 3a. The average diameter for the particles is about 1281 ± 192 nm. The LSAF:Mn was taken to investigate the elemental composition by energy dispersive spectrometry (EDS) as given in Fig. 3b. The EDS spectrum indicates that the composing element F, Sr, Al, and Mn atoms were detected, but the element Li is too light to be detected. The results indicate the flaky particles of the phosphor are confirmed to be pure LSAF:Mn. The scanning electron microscopy (SEM) images of LSAF:Mn shown in Fig. 3b (inset) exhibit that the samples consist of flaky particles about 1-3 μm in diameter.

To further confirm the morphology of the as-synthesize samples, the TEM, HRTEM, and elemental mapping were carried out and shown in Fig. 4a-c. In HRTEM, the lattice fringes are found to be about 0.1499 nm, which is consistent with the d-spacing of the (118) plane of LSAF crystal. The mapping images clearly show that the elements present in the synthesized sample are Sr, Al, F, and Mn, which further provides proof that the obtained samples are pure LSAF phases, and Mn^{4+} ions have

been successfully doped into the host lattice.

The thermal stability of phosphor is a key parameter specially for LEDs with high power because its working temperature could arrive at 150 °C, which seriously affect the performance of LEDs, such as the serving lifetime, color rendering index, chromaticity, and luminous efficiency. As shown in Fig. 5a, TG and DTA curves of LSAF:Mn show that the weight has remained the constant until about 760 °C. Such high decomposition temperature suggests that the phosphor LSAF:Mn has high thermal stability and meets the requirement in WLED devices. The diffuse reflection spectra have been recorded for both undoped and Mn⁴⁺ doped LSAF as shown in Fig. 5b. According to the spectra, it can be seen that the two absorption bands peaking at 370 nm and 465 nm are assigned to the spin-allowed ${}^4A_{2g} \rightarrow {}^4T_{1g}$ and ${}^4A_{2g} \rightarrow {}^4T_{2g}$ transitions of Mn⁴⁺, respectively. The strong absorption band between 200~250 nm is originating from the absorption of hosts which found in both curves.

Fig. 6 illustrates the PL spectra of the red phosphor LSAF:Mn measured at 78 and 298 K, respectively. The room-temperature excitation spectrum monitored at 618 nm shows two bands ranging from 300 nm to 500 nm. The bands centered at 365 and 467 nm are owing to ${}^4A_{2g} \rightarrow {}^2T_{1g}$ and ${}^4A_{2g} \rightarrow {}^2T_{2g}$ transitions, respectively.¹⁸ The excitation spectrum demonstrates that LSAF:Mn phosphors could be well excited by blue LED chips. It is worth noting that the spectral overlap between the excitation spectrum of the red phosphor LSAF:Mn and the emission spectrum of the yellow phosphor YAG:Ce is small, the photon reabsorption effect is smaller than nitride red phosphors when they are co-coating on LED chips. Under excitation at 467 nm, the

room-temperature emission spectrum of LSAF:Mn presents six emission peaks at 595, 605, 610, 618, 628, 632, and 646 nm, which belongs to anti-stokes vibronic transitions $\nu_3(t_{1u})$, $\nu_4(t_{1u})$, and $\nu_6(t_{2u})$, zero phonon line (ZPL), and Stokes vibronic transitions $\nu_6(t_{2u})$, $\nu_4(t_{1u})$, and $\nu_3(t_{1u})$, respectively.²⁴ Compared to that measured at 298 K, the emission spectrum measured at 78 K represents blue-shift in all the Stokes vibronic transitions of Mn^{4+} ions mainly due to a nephelauxetic effect aroused by unit cell shrinkage.¹³ The decreased absorbed photons and less weak vibration transition coupling associated with the vibration modes of $[MnF_6]^{2-}$ octahedron at lower temperature also contribute the blue-shift in emitting transitions of Mn^{4+} ions. The zero phonon line (ZPL) of Mn^{4+} ions is generally locating >620 nm, such as at 625 nm in K_2LiAlF_6 and 620 nm in Na_3AlF_6 , which indicates red shift compared to the ZPL at 618 nm in the emission spectrum of LSAF:Mn measured at 298 K.^{23,24} The ZPL emission intensity depends on the local symmetry of sites that the Mn^{4+} ion occupied. The distortion of the octahedron and the low symmetry will lead to the stronger ZPL emission of Mn^{4+} ion.²⁴⁻²⁵ The location of ZPL of the Mn^{4+} might be attributed to the crystal field strength and bond strength of Al-F bond in $[AlF_6]^{3-}$ octahedron. The electron deficiency of divalent Sr^{2+} ions is stronger than that of monovalent alkaline metal ions such as K^+ and Na^+ in previous works, which leads to lower electron cloud density and shorter Al-F bond length in LSAF than those in K_2LiAlF_6 and Na_3AlF_6 .^{23,24} Therefore, the wavelength of ZPL emission in LSAF is shorter than that in alkaline metal fluoaluminates due to the stronger crystal field strength aroused by Sr^{2+} ions in LSAF.

According to the method reported previously, the ratio of Dq/B is 3.88 that is higher than 2.2, indicating that Mn^{4+} ions experience a strong crystal field LSAF host lattice.^{12,26} The Dq/B value in the $LiNa_2AlF_6$ host lattice is 3.80 according to the data in previous work, which is smaller than that in LSAF.¹² The result demonstrates the crystal field in LSAF is stronger than that in $LiNa_2AlF_6$. The 2E_g level of Mn^{4+} ion is almost independent of the crystal field strength according to the Tanabe-Sugano energy level diagram. Whereas the emission peak energy ${}^2E_g \rightarrow {}^4A_{2g}$ transition of Mn^{4+} depends mainly on the nephelauxetic effect, which is mainly derived from the covalent value of Mn^{4+} -ligand bonding.²⁷ The as-prepared powder sample LSAF:Mn is white under natural light and emits intense red luminescence under UV lamp as shown in their photographs in Fig. 6b (inset), indicates that this red-emitting phosphor can be used as a red component applied to LED technology. On the basis of the emission spectrum of LSAF:Mn, the CIE chromaticity coordinate of LSAF:Mn are calculated as $x = 0.680$ and $y = 0.318$.

3.2 Optimized luminescence and concentration quenching mechanism

Fig. 7a shows the emission spectra for a series of LSAF: xMn ($x = 0.5-16$ mol%), in which, x is the ratio of $K_2MnF_6/LSAF$. All of the spectra have identical features except for their emission intensity. It is clearly that the luminescence intensity of LSAF:Mn increases initially and reaches a maximum at $x = 2$ mol%, then decrease, which is ascribe to concentration quenching. The luminescence decay curves of LSAF:Mn with different concentrations of Mn^{4+} monitored at 618 nm and recorded under excitation at 467 nm at room-temperature are shown in Fig. 7b. All the decay

curves could be well fitted into singly exponential function as:²⁸⁻³⁰

$$I_t = I_0 \exp(-t / \tau) \quad (3)$$

Where I_0 and I_t are for the luminescence intensities at time t_0 and t_t , respectively; τ denotes the decay time of luminescence from corresponding sample, which could be easily calculated by fitting the decay curves. With the ratio of $\text{K}_2\text{MnF}_6/\text{LSAF}$ increasing from 0.5 to 16 mol%, the lifetime decreases from 4.11 to 3.35 ms.

Concentration quenching is usually caused by the occurrence of energy transfer between the nearest Mn^{4+} ions. Since there is no overlap between the excitation and emission spectra of Mn^{4+} ions, the energy transfer mechanism involved in the LSAF crystal host is not radiation reabsorption. It may be due to exchange interaction or electric multipolar interaction. Since there is only one kind of Mn^{4+} luminescent center in the host lattice, the critical energy transfer distance (R_c) between Mn^{4+} ions can be calculated by the following equation:^{13,14}

$$R_c \approx 2 \left[\frac{3V}{4\pi x_c N} \right]^{1/3} \quad (4)$$

Where V is the volume of the unit cell, x_c is the critical concentration of the activator ion, and N is the number of formula units per unit cell. For LSAF host lattice, $V = 228.7 \text{ \AA}^3$, $N = 2$, and the critical concentration of Mn^{4+} is found to be 2 mol%. Therefore, R_c of Mn^{4+} is determined to be 22.19 \AA . Non-radiative energy transfer among Mn^{4+} ions usually occurs as a result of an exchange interaction, radiation reabsorption, or a multipole-multipole interaction.

The exchange interaction responsible for the energy transfer for spin-allowed

transition of Mn^{4+} ion is excluded because R_c of Mn^{4+} in LSAF:Mn is much larger than 5 Å. In view of the little overlapping of emission and excitation spectrum of LSAF:Mn phosphor, the reabsorption mechanism should not occur in this case. Therefore, the multipole-multipole interaction is dominant for the concentration quenching mechanism of Mn^{4+} emission in LSAF:Mn.

Generally, elevating reaction temperature is favorable to gain higher luminescence efficiency for traditional rare earth ions doped inorganic phosphor.^{31,32} We obtained a series of LSAF:Mn samples at a reaction temperature ranging from 25 to 200 °C. All the samples are confirmed to be pure LSAF phase as shown in Fig. 1 and emit red light as shown in emission spectra in Fig. 8. All the emission spectra have similar features and their integrated luminescence intensities depend strongly on the reaction temperature. With the reaction temperature increasing, the luminescence intensity increases and reaches a maximum at 50 °C, then decreases with reaction temperature further increasing. The results indicate elevating reaction temperature to 50 °C can improve the luminescence intensity of LSAF:Mn slightly which might be due to the improvement of crystallization. Whereas, further increasing reaction temperature to be higher than 80 °C will lead to decomposing of K_2MnF_6 and decrease the concentration of luminescence centers.³³⁻³⁶ Consequently, the doping and crystallization of Mn^{4+} doped fluorides can be actually completed at room-temperature and their formation mechanism based on dynamically ion exchange is quite different from that for the traditional rare earth ions doped phosphors. The typical internal quantum yield of the sample LSAF:Mn is about 78% measured according to the method used in the

previous works.¹²

3.3 Temperature-dependent luminescence and thermal quenching

The thermal quenching of luminescence is an important parameter to evaluate the performance of phosphor materials. Fig. 9a depicts the dependence of luminescence of LSAF:Mn on measurement temperature. With increasing temperature, the emission intensity decreases gradually due to the temperature quenching. Note that the intensity at 493 K still remains over 55% of that at room-temperature.

4. Conclusion

In conclusion, we explored a novel red fluoride phosphor LSAF:Mn including strontium at room-temperature. The obtained phosphor LSAF:Mn shows broadened excitation band around 470 nm, and enhanced red emissions due to the spin forbidden transitions ${}^2E_g \rightarrow {}^4A_{2g}$ of Mn^{4+} . The chromaticity coordinates for phosphor LSAF:Mn are located at $x=0.68$ and $y=0.32$, which are very close to standard red region (0.67, 0.33). The optimal concentration of K_2MnF_6 in the reaction system is 2.0 mol% of LSAF and the optimal experimental temperature is 50 °C to obtain the highest luminescent intensity. The red phosphor LSAF:Mn keep undecomposed up to 700 °C which indicates excellent thermal stability and a suitable candidate for the fabrication of blue InGaN based WLEDs.

Acknowledgments

This research was jointly supported by the National Natural Science Foundation of China (Grant No. 51572200, 51672266, 51628201, and 91433110), Zhejiang Province (Grant No. Y16E020041), and the Public Industrial Technology Research Projects of Wenzhou (Grant No. G20170005) and the Joint Project of National Natural Science

Foundation of China (NSFC) and Yunnan Province (U1702254).

References

- [1] Z.G. Xia, Z.H. Xu, M.Y. Chen, Q.L. Liu, Recent developments in the new inorganic solid-state LED phosphors, *Dalton Trans.* 45 (2016) 11214-11232.
- [2] G.G. Li, Y. Zhao, Y. Wei, Y. Tian, Z.W. Quan, J. Lin, Novel yellowish-green light-emitting $\text{Ca}_{10}(\text{PO}_4)_6\text{O}:\text{Ce}^{3+}$ phosphor: structural refinement, preferential site occupancy and color tuning *Chem. Commun.* 52 (2016) 3376-3379.
- [3] Y.H. Kim, P. Arunkumar, B.Y. Kim, S. Unithrattil, E. Kim, S.H. Moon, J.Y. Hyun, K.H. Kim, D. Lee, J.S. Lee, W.B. Im, A zero-thermal-quenching phosphor, *Nat. Mater.* 16 (2017) 543.
- [4] X. Ding, G. Zhu, W.Y. Geng, Q. Wang, Y.H. Wang, Rare-earth-free high-efficiency narrow-band red-emitting $\text{Mg}_3\text{Ga}_2\text{GeO}_8:\text{Mn}^{4+}$ phosphor excited by near-UV light for white-light-emitting diodes, *Inorg. Chem.* 55 (2016) 154-162.
- [5] X. Ding, Q. Wang, Y.H. Wang, Rare-earth-free red-emitting $\text{K}_2\text{Ge}_4\text{O}_9:\text{Mn}^{4+}$ phosphor excited by blue light for warm white LEDs, *Phys. Chem. Chem. Phys.* 18 (2016) 8088-8097.
- [6] W.B. Im, N. George, J. Kurzman, S. Brinkley, A. Mikhailovsky, J. Hu, B.F. Chmelka, S.P. DenBaars, R. Seshadri, Efficient and color - tunable oxyfluoride solid solution phosphors for solid - state white lighting, *Adv. Mater.* 23 (2011) 2300-2305.
- [7] Z.G. Xia, Q.L. Liu, Progress in discovery and structural design of color

- conversion phosphors for LEDs, *Prog. Mater. Sci.* 84 (2016) 59-117.
- [8] N.C. George, K.A. Denault, R. Seshadri, Phosphors for solid-state white lighting, *Annu. Rev. Mater. Res.* 43 (2013) 481-501.
- [9] H.M. Zhu, C.C. Lin, W.Q. Luo, S.T. Shu, Z.G. Liu, Y.S. Liu, J.T. Kong, E. Ma, Y.G. Cao, R.S. Liu, X.Y. Chen, Highly efficient non-rare-earth red emitting phosphor for warm white light-emitting diodes, *Nat. Commun.* 5 (2014) 4312.
- [10] M.H. Fang, H.D. Nguyen, C.C. Lin, R.S. Liu, Preparation of a novel red $\text{Rb}_2\text{SiF}_6:\text{Mn}^{4+}$ phosphor with high thermal stability through a simple one-step approach, *J. Mater. Chem. C* 3 (2015) 7277-7280.
- [11] M.M. Zhu, Y.X. Pan, L.Q. Xi, H.Z. Lian, J. Lin, Design, preparation, and optimized luminescence of a dodec-fluoride phosphor $\text{Li}_3\text{Na}_3\text{Al}_2\text{F}_{12}:\text{Mn}^{4+}$ for warm WLED applications, *J. Mater. Chem. C* 5 (2017) 10241-10250.
- [12] M.M. Zhu, Y.X. Pan, Y.Q. Huang, H.Z. Lian, J. Lin, Designed synthesis, morphology evolution and enhanced photoluminescence of a highly efficient red dodec-fluoride phosphor, $\text{Li}_3\text{Na}_3\text{Ga}_2\text{F}_{12}:\text{Mn}^{4+}$ for warm WLEDs, *J. Mater. Chem. C* 6 (2018) 491-499.
- [13] Y.W. Zhu, L.Y. Cao, M.G. Brik, X.J. Zhang, L. Huang, T.T. Xuan, J. Wang, Facile synthesis, morphology and photoluminescence of a novel red fluoride nanophosphor $\text{K}_2\text{NaAlF}_6:\text{Mn}^{4+}$, *J. Mater. Chem. C* 5 (2017) 6420-6426.
- [14] Y.W. Zhu, L. Huang, R. Zou, J.H. Zhang, J.B. Yu, M.M. Wu, J. Wang, Q. Su, Hydrothermal synthesis, morphology and photoluminescent properties of an Mn^{4+} -doped novel red fluoride phosphor elpasolite K_2LiAlF_6 , *J. Mater. Chem. C*

4 (2016) 5690-5695.

- [15] D. Sekiguchi, S. Adachi, Synthesis and optical properties of BaTiF₆: Mn⁴⁺ red phosphor, ECS J. Solid State Sci. Tech. 3 (2014) R60-R64.
- [16] X.L. Gao, Y. Song, G.X. Liu, X.T. Dong, J. Wang, W.S. Yu, Narrow-band red emitting phosphor BaTiF₆:Mn⁴⁺: preparation, characterization and application for warm white LED devices, Dalton Trans. 45 (2016) 17886-17895.
- [17] X.Y. Jiang, Y.X. Pan, S.M. Huang, X. Chen, J.G. Wang, G.K. Liu, Hydrothermal synthesis and photoluminescence properties of red phosphor BaSiF₆:Mn⁴⁺ for LED applications, J. Mater. Chem. C 2 (2014) 2301-2306.
- [18] H.Z. Lian, Q.M. Huang, Y.Q. Chen, K. Li, S.S. Liang, M.M. Shang, M.M. Liu J. Lin, Resonance Emission Enhancement (REE) for Narrow Band Red-Emitting A₂GeF₆:Mn⁴⁺ (A = Na, K, Rb, Cs) Phosphors Synthesized via a Precipitation–Cation Exchange Route, Inorg. Chem. 56 (2017) 11900-11910.
- [19] L.Q. Xi, Y.X. Pan, M.M. Zhu, H.Z. Lian, J. Lin, Abnormal site occupancy and high performance in warm WLEDs of a novel red phosphor, NaHF₂:Mn⁴⁺, synthesized at room temperature, Dalton Trans. 46 (2017) 13835-13844.
- [20] Q. Zhou, Y.Y. Zhou, Y. Liu, Z.L. Wang, G. Chen, J.H. Peng, J. Yan, M.M. Wu, A new and efficient red phosphor for solid-state lighting:Cs₂TiF₆:Mn⁴⁺, J. Mater. Chem. C 3 (2015) 9615-9619.
- [21] L.L. Wei, C.C. Lin, M.H. Fang, M.G. Brik, S.F. Hu, H. Jiao, R.S. Liu, A low-temperature co-precipitation approach to synthesize fluoride phosphors K₂MF₆:Mn⁴⁺ (M = Ge, Si) for white LED applications, J. Mater. Chem. C 3

(2015) 1655-1660.

- [22] T.F. Antokhina, S.B. Ivanov, N.N. Savchenko, L.V. Teplukhina, Synthesis and physicochemical study of hexafluorocomplexes of tin with mixed alkali metal cations, *Bull. Acad. Sci., Divi.Chem. Sci.* 36 (1987) 1785-1789.
- [23] Y.W. Zhu, Y. Liu, L. Huang, T.T. Xuan, J. Wang, Optimized photoluminescence of red phosphor $\text{K}_2\text{LiAlF}_6:\text{Mn}^{4+}$ synthesized by a cation-exchange method, *Sci. China Technol. Sc.* 60 (2017) 1458-1464.
- [24] E.H. Song, J.Q. Wang, S. Ye, X.F. Jiang, M.Y. Peng, Q.Y. Zhang, Room-temperature synthesis and warm-white LED applications of Mn^{4+} ion doped fluoroaluminate red phosphor $\text{Na}_3\text{AlF}_6:\text{Mn}^{4+}$, *J. Mater. Chem. C* 4 (2016) 2480-2487.
- [25] L.L. Wei, C.C. Lin, Y.Y. Wang, M.H. Fang, H. Jiao, R.S. Liu, Photoluminescent evolution induced by structural transformation through thermal treating in the red narrow-band phosphor $\text{K}_2\text{GeF}_6:\text{Mn}^{4+}$, *ACS Appl. Mater. Inter.* 7 (2015) 10656-10659.
- [26] Y.H. Jin, Y.H. Hu, H.Y. Wu, H. Duan, L. Chen, Y.R. Fu, G.F. Ju, Z.F. Mu, M. He, A deep red phosphor $\text{Li}_2\text{MgTiO}_4:\text{Mn}^{4+}$ exhibiting abnormal emission: potential application as color converter for warm w-LEDs, *Chem. Eng. J.* 288 (2016) 596-607.
- [27] M. G. Brik, A. M. Srivastava, On the optical properties of the Mn^{4+} ion in solids, *ECS J. Solid State Sci. Technol.* 2 (2013) R148.

- [28] K. Li, D.Q. Chen, R. Zhang, Y.L. Yu, Y.S. Wang, $\text{Eu}^{2+}:\text{SrMg}_{1-x}\text{Mn}_x\text{P}_2\text{O}_7$ ($x = 0-1$) phosphors with tunable yellow-red emissions, *J. Alloy. Compd.*, 555 (2013) 45-50.
- [29] X.L. Tan, M. Fang, L.Q. Tan, H.N. Liu, X.S. Ye, T. Hayat, X.K. Wang, Core-shell hierarchical $\text{C}@\text{Na}_2\text{Ti}_3\text{O}_7 \cdot 9\text{H}_2\text{O}$ nanostructures for the efficient removal of radionuclides, *Environ. Sci. Nano*, 5 (2018) 1140-1149.
- [30] M.G. Kong, M. Fang, X.L. Tan, M. Liu, G.L. Shang, G.T. Fei, L.D. Zhang, The investigation on the mechanism of the increased decay time in red $\text{SrS}:\text{Eu}^{2+}, \text{Dy}^{3+}$ phosphor, *Mater. Chem. Phys.*, 207 (2018) 161-166.
- [31] X.Y. Bao, S.P. Zhou, J.G. Wang, L.J. Zhang, S.M. Huang, Y.X. Pan, Color tunable phosphor $\text{CaMoO}_4:\text{Eu}^{3+}, \text{Li}^+$ via energy transfer of $\text{MoO}_4^{2-}-\text{Eu}^{3+}$ dependent on morphology and doping concentration, *Mater. Res. Bull.* 48 (2013) 1034-1039.
- [32] Y.X. Pan, M.M. Wu, Q. Su, Comparative investigation on synthesis and photoluminescence of $\text{YAG}:\text{Ce}$ phosphor, *Mater. Sci. Engin. B* 106 (2004) 251-256.
- [33] L. Huang, Y.W. Zhu, X.J. Zhang, R. Zou, F.J. Pan, J. Wang, M.M. Wu, HF-free hydrothermal route for synthesis of highly efficient narrow-band red emitting phosphor $\text{K}_2\text{Si}_{1-x}\text{F}_6:x\text{Mn}^{4+}$ for warm white light-emitting diodes, *Chem. Mater.* 28 (2016) 1495-1502.
- [34] L.F. Lv, Z. Chen, G.K. Liu, S.M. Huang, Y.X. Pan, Optimized photoluminescence of red phosphor $\text{K}_2\text{TiF}_6:\text{Mn}^{4+}$ synthesized at room temperature and its formation mechanism, *J. Mater. Chem. C*, 3 (2015) 1935-1941.

- [35] L.Q. Xi, Y.X. Pan, M.M. Zhu, H.Z. Lian, J. Lin, Room-temperature synthesis and optimized photoluminescence of a novel red phosphor $\text{NaKSnF}_6:\text{Mn}^{4+}$ for application in warm WLEDs, *J. Mater. Chem. C* 5 (2017) 9255-9263.
- [36] L.Q. Xi, Y.X. Pan, X. Chen, S.M. Huang, M.M. Wu, Optimized photoluminescence of red phosphor $\text{Na}_2\text{SnF}_6:\text{Mn}^{4+}$ as red phosphor in the application in “warm” white LEDs, *J. Am. Ceram. Soc.* 100 (2017) 2005-2015.

Figure captions:

Fig. 1 XRD patterns of samples prepared (a) at different temperatures with molecular ratio of $\text{K}_2\text{MnF}_6/\text{LiSrAlF}_6 = 2$ mol% and (b) with various molecular ratios of $\text{K}_2\text{MnF}_6/\text{LiSrAlF}_6$.

Fig. 2 X-ray diffraction patterns of $\text{LiSrAlF}_6:\text{Mn}^{4+}$ samples (a) obtained after full-pattern Rietveld refinement and (b) the structure projection of $\text{LiSrAlF}_6:\text{Mn}^{4+}$ crystal structure plotted by software Diamond 3.1.

Fig. 3 (a) Size distribution and (b) EDS spectrum of $\text{LiSrAlF}_6:\text{Mn}^{4+}$ particles (inset: SEM images of $\text{LiSrAlF}_6:\text{Mn}^{4+}$ flaky particles).

Fig. 4 (a) TEM, (b) HRTEM images, and (c) the element mapping of Sr, Al, F, and Mn in selected area of $\text{LiSrAlF}_6:\text{Mn}^{4+}$ sample.

Fig. 5 (a) The thermogravimetrics (TG) analysis and different scanning calorimeter (DSC) of red phosphor $\text{LiSrAlF}_6:\text{Mn}^{4+}$ and (b) the diffuse reflectance spectra of undoped LiSrAlF_6 and red phosphors $\text{LiSrAlF}_6:\text{Mn}^{4+}$.

Fig. 6 (a) Excitation and (b) emission spectra of $\text{LiSrAlF}_6:\text{Mn}^{4+}$ with molecular ratio of $\text{K}_2\text{MnF}_6/\text{LiSrAlF}_6 = 2$ mol% measured at 78 and 298 K, respectively. (Inset: photographs of the phosphor $\text{LiSrAlF}_6:\text{Mn}^{4+}$ taken under visible light and UV light, respectively.)

Fig. 7 (a) Emission spectra (inset: dependence of integrated emission intensity on the concentrations of K_2MnF_6 .) and (b) decay curves for red emission of phosphor $\text{LiSrAlF}_6:\text{Mn}^{4+}$ prepared with various concentrations of K_2MnF_6 .

Fig. 8 Emission spectra and the corresponding integrated luminescence intensity of

LiSrAlF₆:Mn⁴⁺ with molecular ratio of K₂MnF₆/LiSrAlF₆ = 2 mol% dependent on reaction temperature.

Fig. 9 (a) The emission spectra and (b) the luminescence intensity of LiSrAlF₆:Mn⁴⁺ with molecular ratio of K₂MnF₆/LiSrAlF₆ = 2 mol% dependent on measurement temperature.

Figures:

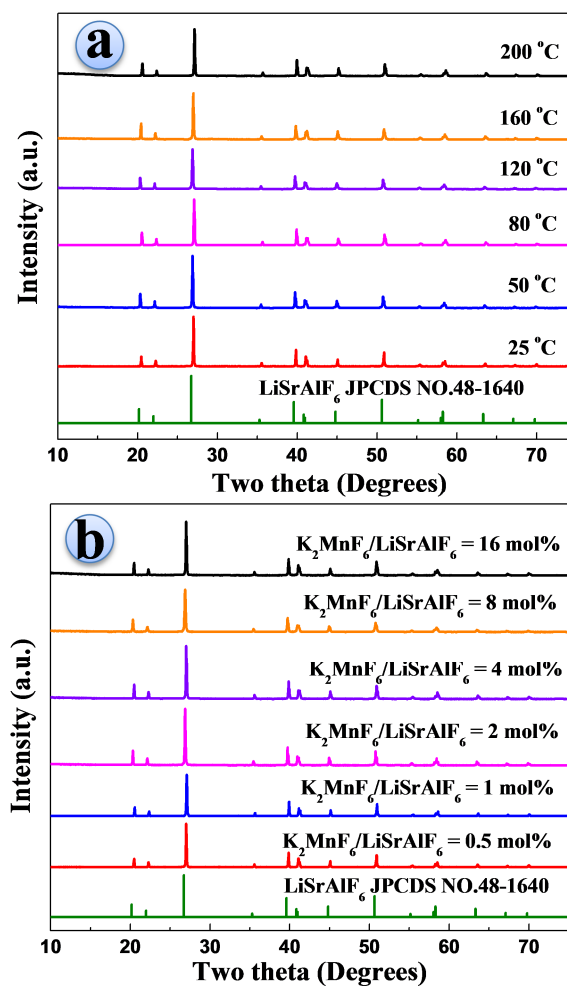


Fig. 1

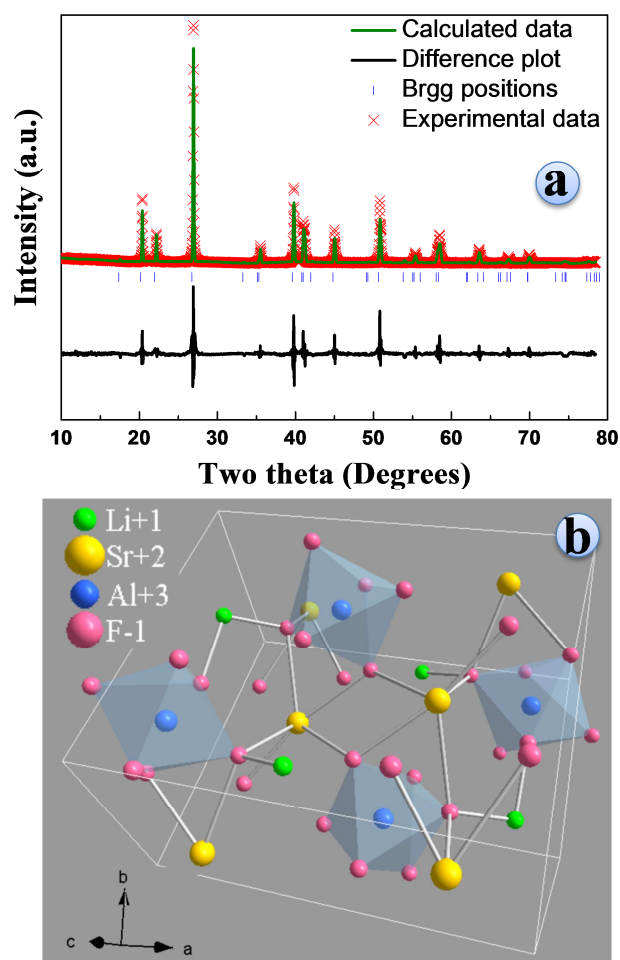


Fig. 2

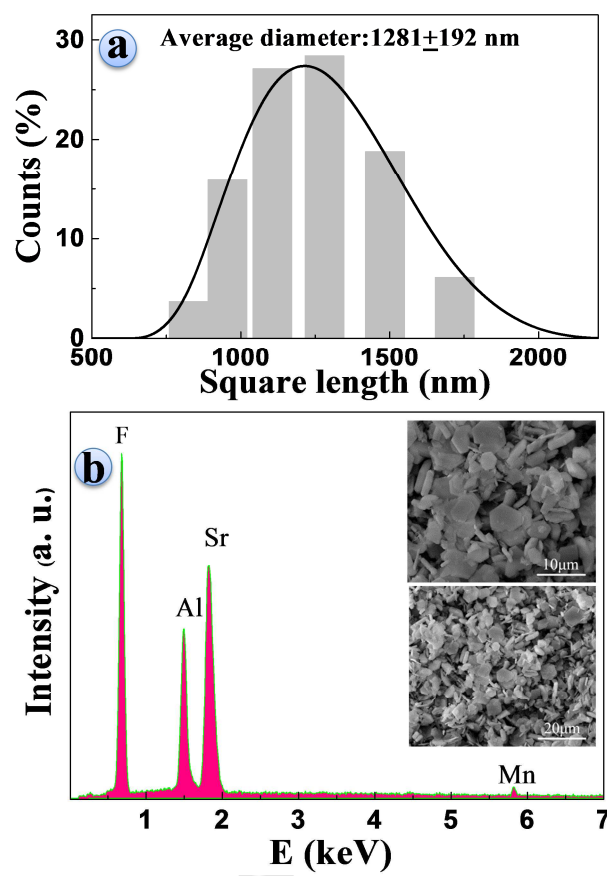


Fig. 3

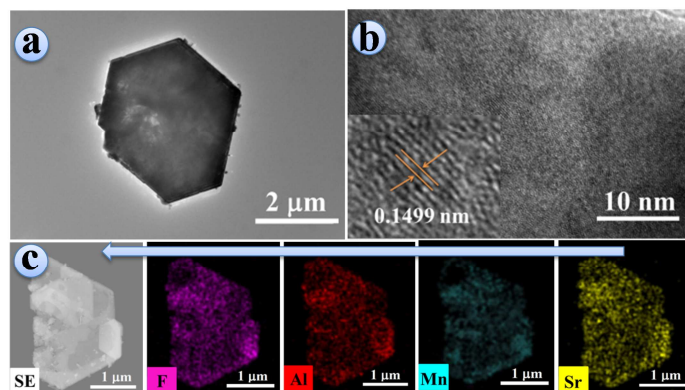


Fig. 4

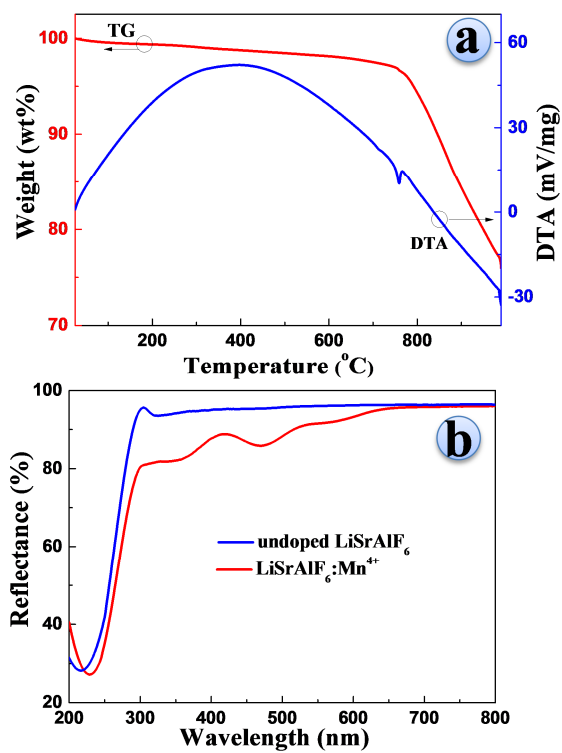


Fig. 5

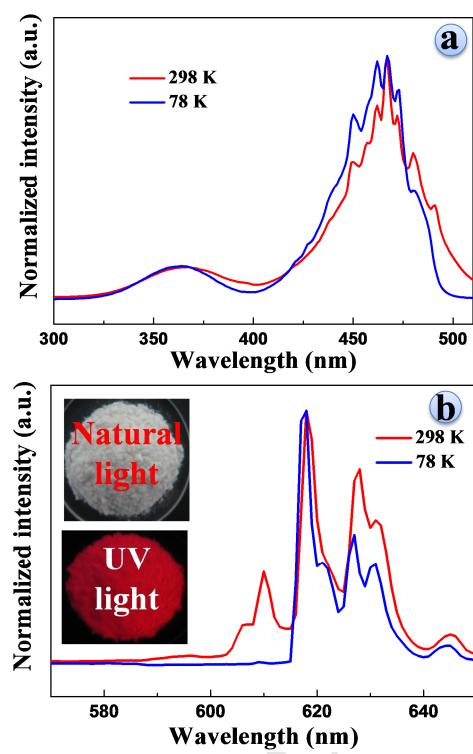


Fig. 6

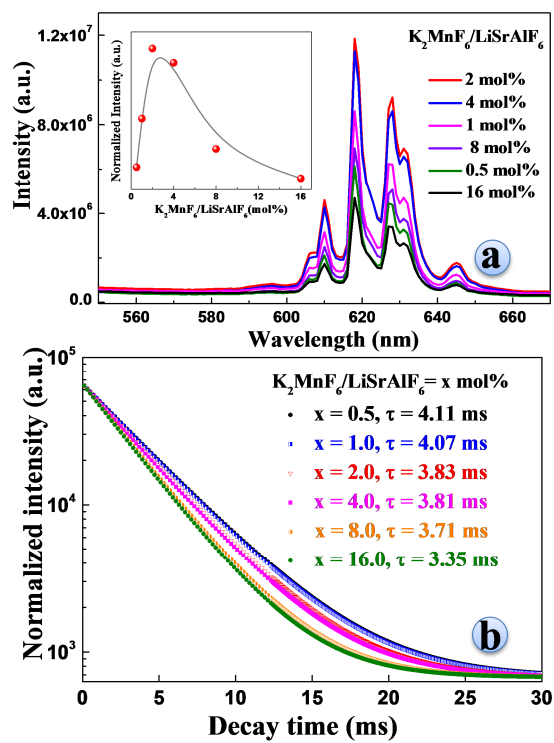


Fig. 7

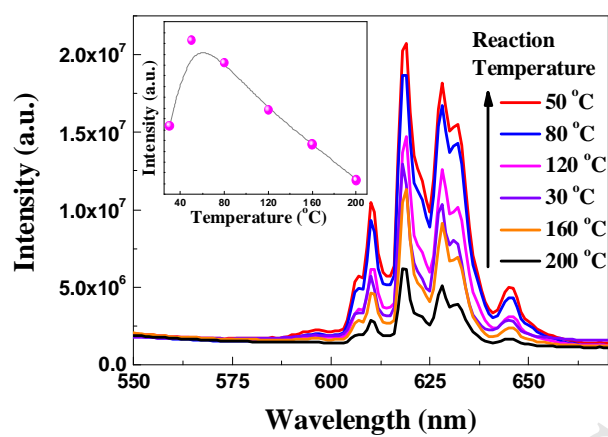


Fig. 8

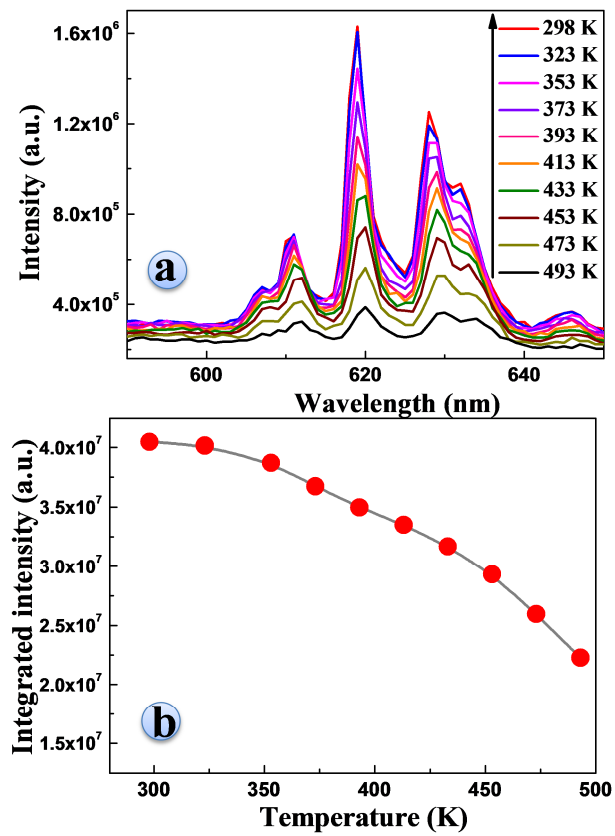


Fig. 9

Table 1 Refined structural parameters for $\text{LiSrAlF}_6:\text{Mn}^{4+}$ at room temperature.

Atoms	site	Occupancy	x	y	z	Biso(\AA^2)
Li1	2c	1	0.3333	0.6667	0.25	1.34(1)
Sr1	2b	1	0	0	0	1.54(1)
Al1/Mn1	2d	0.98/0.02	0.6667	0.3333	0.25	1.42(1)
F1	12i	1	0.3892(8)	0.027(1)	0.1475(5)	1.72(1)

a = b = 5.071 \AA , c = 10.189 \AA , V = 226.91 \AA^3 , space group: P-31c(163), Z = 2;
refinement result: $R_{\text{WP}} = 5.24\%$, $R_{\text{P}} = 11.14\%$, $\chi^2 = 3.03$

Highlights.

1. Synthesis of $\text{LiSrAlF}_6:\text{Mn}^{4+}$ at room temperature and its reaction mechanism.
2. The phosphor shows good thermal stability and optical properties.
3. The influence of synthesis conditions on luminescence is studied.